Preparation of cellulose nanocrystal-reinforced keratin bioadsorbent for highly effective and recyclable removal of dyes from aqueous solution

Kaili Song,[a,b] Helan Xu,[b] Lan Xu,[c] Kongliang Xie,[a] Yiqi Yang [b,d,e]*

[a]Key Laboratory of Science and Technology of Eco-Textiles, Ministry of Education, College of Chemistry, Chemical Engineering and Biotechnology, Donghua University, Shanghai 201620, China

[b]Department of Textiles, Merchandising and Fashion Design, 234, HECO Building, University of Nebraska-Lincoln, Lincoln, NE 68583-0802, United States

[c]Department of Agronomy and Horticulture, University of Nebraska-Lincoln, Lincoln, NE 68583-0915, United States

[d]Department of Biological Systems Engineering, 234, HECO Building, University of Nebraska-Lincoln, Lincoln, NE 68583-0802, United States

[e]Nebraska Center for Materials and Nanoscience, 234, HECO Building, University of Nebraska-Lincoln, Lincoln, NE 68583-0802, United States

* Corresponding Author. Tel: +001 402 472 5197; Fax: +001 402 472 0640;

E-mail: yyang2@unl.edu

Abstract

High-efficiency and recyclable three-dimensional bioadsorbents were prepared by incorporating cellulose nanocrystal (CNC) as reinforcements in keratin sponge matrix to remove dyes from aqueous solution. Adsorption performance of dyes by CNC-reinforced keratin bioadsorbent was improved significantly as a result of adding CNC nano-filler. Batch adsorption results showed that the adsorption capacities for Reactive Black 5 and Direct Red 80 by the bioadsorbent were 1201 and 1070 mg g^{-1}, respectively. The adsorption isotherms and kinetics for adsorption of both dyes on bioadsorbent followed the Langmuir isotherm model and pseudo-second order model, respectively. Desorption and regeneration experiments showed that the removal efficiencies of the bioadsorbent for both dyes could remain above 80% at the fifth recycling cycles. Moreover, the bioadsorbent possessed excellent packed-bed column operation performance. Those results suggested that the adsorbent could be considered as a high performance and promising candidate for dye wastewater treatment.

Keywords**:** keratin adsorbent; cellulose nanocrystal; adsorption; dye wastewater treatment.

1. Introduction

Global occurrence of environmental pollution caused by industrial wastewater has raised more and more concerns since it seriously hinders the sustainable and continuous development of society (Qin et al., 2016; Zhao et al., 2015). Treatment of wastewater discharged form textile dyeing is among the most challenging ones (Tao et al., 2016; Wang et al., 2016). It was estimated over 7×10^5 tons of dyes and pigments are produced annually and about 10–25% of them are discharged into environment during their applications (Papić et al., 2004). Due to the complex structures of dye, they are usually stable and non-biodegradable in the environment (Xu et al., 2013; Zou et al., 2010). More seriously, some of the organic dyes are even teratogenetic and carcinogenic, which create serious threats to marine organisms as well as human beings

(Maneerung et al., 2016; Paletal, 2015). Thus, it is imperative to treat dye effluents in order to protect environment and preserve a virtuous cycle of aquatic ecosystem.

Recently, numerous dye wastewater treatment technologies, such as photo-degradation, coagulation, advanced oxidation, electrochemical degradation, membrane filtration and so on, have been developed (Yao et al., 2015; Gupta and Suhas, 2009; Crini, 2006). However, due to either the high cost or the practical unfeasible those technologies, adsorption is considered to be the most promising and technically feasible method as for its relatively low cost, flexibility and simplicity of operation. Numerous studies on adsorption removal of dye from effluents have been witnessed recently (González et al., 2015; Lin et al., 2013; Liu et al., 2015; Nair and Vinu, 2016; Yao et al., 2015; Zhang et al., 2017). It has been reported that 3741 bio-sorption papers were published from the period of 2013 to the end of May 2016 worldwide based on search result from Web of Science (Liu and Lee, 2014). Despite of those extensive attempts for development of adsorbent from various sources for dye wastewater treatment, the problem is still a tough issue and little progress had been made for practical application either due to the low adsorption capacity or difficulty in regeneration as well as the relatively high cost (Lu and Gibb, 2008). Therefore, it is still challenging to address those issues and highly demanding to develop adsorbents with high adsorption performance, easy regeneration and cost effective for environmental remediation. During the pursuit of high performance adsorbent, those bioadsorbent derived from bio-based feedstocks or biomass co-productions such as rice husk, straw, cotton stalk, poultry feather and food scraps are receiving more and more attention due to their low cost and naturally abundance. (Achak et al., 2009; Aluigi et al., 2014; Bilal et al., 2013; Cazetta et al., 2015).

Keratin, being the major component of feathers, wools, animal nails and hairs, is an abundant and non-food protein characterized by large numbers of functional groups such as carboxyl, amino groups on its molecules which could act as adsorption site for dyes (Xu et al., 2014). Moreover, keratin could be largely obtained from butchery wastes such as feathers, horns-nails, and poor quality wools or used fabrics from textile industry. Thus, it is suitable to be exploited as adsorbent for water treatment. Keratin sponges which exhibit high porosity and specific surface area is more desirable to be applied in water treatment. Unfortunately, the weak mechanical property of keratin sponge is the most serious problem that hinders its wide application. To address this drawback, numerous investigations have been carried out by incorporating of nano-filler including carbon nanotube (Song et al., 2015), clay (Yang et al., 2011), graphene sheets (Huang et al., 2016) and so on, as reinforcement to improve mechanical property of the matrix. Among those nano-fillers, cellulose nanocrystals (CNC) which have ordered crystalline region, high Young's modulus (up to 140 GPa), as well as large surface area ($\sim$700 m^2 g^{-1}) have attracted increasing interests recently as reinforcing agents.

In this study, we demonstrated a facile strategy to fabricate mechanically strong keratin spongy bioadsorbent by incorporating CNC as reinforcing building blocks, yielding a CNC reinforced 3D keratin bioadsorbent. To the best of our knowledge, this is the first time that CNC reinforced 3D keratin spongy bioadsorbent was prepared and used as adsorbent for dye removal. Its performance for dye removal was systematically studied in batch condition, and its desorption and recyclability were also investigated. Furthermore, we conducted the fixed bed column study to explore its performance in continuous conditions. The results indicated that the CNC reinforced keratin bioadsorbent could be considered as a desirable and promising adsorbent for environmental remediation. The benefit of the strategy in our work includes the following: (1) a

simple process to improve the mechanical property of keratin adsorbent, which is crucial for its regeneration and recycling, (2) the CNC reinforced 3D keratin adsorbent exhibiting high specific surface area and large porosity, (3) owing to the three-dimensional structure and considerable functional groups act as adsorption sites on the surface of the adsorbent, dye molecules can be efficiently adsorbed from aqueous solution.

2. Experimental

2.1. Materials

White chicken feathers were kindly provided by Feather Fiber Corp., Nixa, MO. Sulfuric acid, glutaraldehyde (25% in aqueous solution) were purchased from VWR international, Bristol CT. Cysteine was purchased from EMD Chemicals Inc. Gibbstown, NJ. Urea was purchased from Oak Chemical, Inc. West Columbia, SC. Two commercial dyes, Reactive Black 5 ($C_{26}H_{21}N_5Na_4O_{19}S_6$, RB5) and Direct Red 80 ($C_{45}H_{26}N_{10}Na_6O_{21}S_6$, DR80) obtained from Hoechst Celanese Corporation, Bridgewater, NJ, were used without further treatment and purities of around 75% was considered for calculations. The chemical structures and some properties of RB5 and DR80 are listed in Table S1.

2.2. Preparation of bioadsorbent

Keratin solution was prepared according to the procedure developed previously by our group with minor modification (Xu and Yang, 2014). Briefly, 100 g of chicken feather was immersed in 1700 mL solution containing 8M urea, 10 g cysteine at pH 10.5. The feather dispersion solution was stirred vigorously at 70 °C for 10 h. Keratin solution was collected by centrifuge removing the undissolved feather. After that, the obtained solution was dialyzed against distilled water for 36 h with changing water every 4 h. Cellulose nanocrystal (CNC) was obtained by sulfuric acid (65% wt) hydrolysis of cotton fabric at 45 °C for 45 min at a ratio of 1:30 (cotton to

sulfuric acid solution) according to the reported method with minor modification (Lin et al., 2012). The final concentration of the keratin and CNC solution was measured by dry weight method.

CNC reinforced keratin adsorbent was fabricated by freeze drying. CNC (25% weight ratio of keratin) was added into 1% wt keratin solution and the dispersion was sonicated for 5 min in an ice bath using an ultrasonic processor (VCX 500:500 W, Sonics & Materials, Newton, CT). After that crosslinking agent glutaraldehyde (10% based on the weight of keratin) solution at pH 6.5 was added into the obtained dispersion. The mixture was stirred for 5 min and then put into -80 °C refrigerator for 2 h before freeze-dried for 36 h. The freeze-dried keratin adsorbent was put into 70 °C oven for 1 h to allow the crosslinking reaction.

2.3. Characterization of the bioadsorbent

Morphology of the obtained adsorbent was observed using Field Emission Scanning Electron Microscope (FESEM, S3000N, Hitachi, Inc. Schaumburg, IL). The adsorbent was sputter-coated with gold/palladium and observed at a voltage of 10 kV. Morphology of cellulose nanocrystal was observed using Transmission Electron Microscopy (TEM, Hitachi H7500 transmission electron microscope, Hitachi, Inc., Parlin, NJ). The carboxyl and amine group contents of the adsorbent were determined by conductivity titration using a Mettler Toledo SevenMulti™ S47 pH meter as described previously (Song et al., 2016). Compression strength tests were carried out by TA XT Plus Texture Analyzer (Stable Microsystems Ltd, UK) equipped with two flat-surface compression stages and 10 N load cells. Zeta potential of the adsorbent was measured using a Zeta sizer Nano-ZS90 (Malvern, UK). Water uptake property of the adsorbent was measured by immersing the adsorbent in 1000 mL of distill water at room temperature. The

adsorbents were weighed (W_0) before and after taken out and removing the excess water using a filter water (Wt) at a certain time. The water uptake ratio was calculated using equation (1):

$$Water\ uptake\ (g\ g^{-1}) = \frac{W_t - W_0}{W_0} \qquad (1)$$

The Brunauer−Emmett−Teller areas (BET areas) of the adsorbent were evaluated by BET equation using adsorptionmeter (TriStar 3020, Micromeritics, United States). Porosity of the adsorbent was measured by ethanol displacement method since ethanol is able to fully penetrate into all the pores without changing the geometrical volume and pore structures. A cubic shape (V) of adsorbent (m_1) was immersed into 100 mL of anhydrous ethanol (ρ = 0.789 g mL^{-1}) and then moved into a desiccator that is under reduced pressure for 15 min to remove the air bubbles inside adsorbent before it was taken out. The ethanol on the surface of adsorbent was carefully removed using filter paper. The adsorbent was reweighed (m_2) immediately. The porosity was calculated using the equation (2):

$$\varepsilon\% = \frac{(m_2 - m_1)/\rho}{V} \times 100 \qquad (2)$$

2.4. Batch adsorption experiments

Effect of pH on the removal efficiency and adsorption capacity was investigated in a range of 2 to 11 (considering the properties of real textile dye effluents) at 200 mL dye solution (dye concentration: 200 mg L^{-1}) with 0.1 g adsorbent for 3 h. The effect of adsorbent dosage on the removal efficiency and adsorption capacity was investigated from 0.1 g L^{-1} to 2 g L^{-1} with 200 mL dye solution (dye concentration of 200 mg L^{-1}) at pH 2 for 3 h. Effect of initial dye concentration on the adsorption performance was investigated in a range from 50 to 1500 mg L^{-1} with a bioadsorbent dosage of 0.5 g L^{-1} at pH 2. The effect of contact time (0 to 300 min) was carried out using 200 mL dye solution (dye concentration of 200 mg L^{-1}) with 0.5 g L^{-1} adsorbent dosage at pH 2. The effect of salt on the adsorption performance was also investigated by adding

0-70 g L^{-1} NaCl into 200 mL dye solution (dye concentration of 200 mg L^{-1}) with 0.5 g L^{-1} adsorbent dosage at pH 2. All of the experiments were carried out at room temperature in triplicate. The dye removal efficiency and adsorption capacity was calculated according to the equation (3) and (4):

$$\text{Removal efficiency } (\%) = \frac{C_0 - C_t}{C_0} \times 100 \qquad (3)$$

$$Adsorption\ capacity\ (mg\ g^{-1}) = \frac{(C_0 - C_t) \times V}{m} \times 100 \qquad (4)$$

Where, C_0 and C_t are concentrations of dye in solution at beginning and at time t (mg L^{-1}), respectively. V is the volume of dye solution; m is the weight of adsorbent used.

2.5. Adsorption isotherm and kinetic model

The Langmuir isotherm model is based on the assumption that the adsorbate forms a monolayer coverage on a homogeneous adsorbent surface, whose linear equation is expressed as equation (5):

$$\frac{Ce}{q_e} = \frac{1}{bq_{max}} + \frac{Ce}{q_{max}} \qquad (5)$$

Where, Ce (mg L^{-1}) is the equilibrium concentration of dye; q_e (mg g^{-1}) is the adsorption capacity at equilibrium; q_{max} (mg g^{-1}) is the maximum monolayer adsorption capacity of the adsorbent; b (L mg^{-1}) is the Langmuir constant that relates to the energy and affinity of the adsorbate for the adsorption sites. The Freundlich isotherm model is an empirical formula assumes that multilayer adsorption occurred on a heterogeneous surfaces and non-uniform distribution of adsorption heat over the surface without a saturation of adsorption sites. Its linearized equation is given as equation (6):

$$Lnq_e = LnK_F + \frac{1}{n} LnC_e \qquad (6)$$

Where, K_F is the Freundlich constant and n is the heterogeneity factor, which are related to the adsorption capacity and adsorption intensity, respectively. Another essential parameter, R_L, called the separation factor, is determined by the relation as follows:

$$R_L = \frac{1}{1+bC_0} \qquad (7)$$

where R_L indicates the type of the isotherm to be either unfavorable ($R_L > 1$), linear ($R_L = 1$), favorable ($0 < R_L < 1$), or irreversible ($R_L = 0$).

The pseudo-first-order model assumes that the rate change of adsorbate uptake with time is directly related to the difference in saturation concentrations, while the pseudo-second-order model assumes that the adsorption rate determining step may be a chemical surface reaction. The pseudo-first-order model follows:

$$\ln(q_e - q_t) = lnq_e - k_1 t \qquad (8)$$

The pseudo-second-order model follows:

$$\frac{t}{q_t} = \frac{1}{k_2 q_e^2} + \frac{t}{q_e} \qquad (9)$$

where k_1 (min^{-1}) and k_2 ($mg\ g^{-1}min^{-1}$) are rate constants of pseudo-first-order and pseudo-second-order kinetics equations, respectively. q_t ($mg\ g^{-1}$) is the adsorption capacity at time t, q_e ($mg\ g^{-1}$) is the equilibrium adsorption capacity.

2.6. Recyclability and fixed bed column study

Evaluation of recyclability of the adsorbent was carried out at 0.5 g L^{-1} dosage of bioadsorbent added into 200 mL of 200 mg L^{-1} dye solutions for 300 min, then the adsorbent was taken out from the solution. The desorption and regeneration of the used adsorbent was performed by immersing the adsorbent into 50 mL of 0.1 g L^{-1} NaOH solution with squeeze for 30 min and subsequently washed using distill water till neutral for the next adsorption. The regenerated adsorbent was used for another adsorption study in the subsequent cycles.

Fixed bed column studies were carried out using a glass column with 1.5 cm in the internal diameter and 20 cm high. The adsorbent (0.35 g) was carefully filled into the column after swelling in water for 2 h. The final bed height was 7 cm. The bottom of the column was filled by some small steel ball in order to immobilize the well packed bed. RB5 was chosen as a representative study to evaluate the fixed bed adsorption performance. A concentration of 200 mg L^{-1} RB5 dye solution was pumped downward through the fixed bed at a flow rate of 1 mL min^{-1}. The in situ desorption of the used bed was done by eluting with 0.1 g L^{-1} NaOH solution at a constant flow rate of 0.5 mL min^{-1}. The fixed bed column operation was repeated three times within 3% relative error and the average value was adopted. The concentration of dye solution was measured using a UV/Vis spectrophotometer (Model DU 720, Beckman Coulter Inc., Brea, CA) at wavelength of maximum absorbance, 595 nm and 543 nm for RB5 and DR80, respectively.

2.7. Statistical Analysis

All the obtained data points were compared with the one-way analysis of variance using Scheffé test with the confidence interval of 95%. The p value smaller than 0.05 was used to indicate a satisfied significant difference. Standard deviations are shown in the figures by the error bars.

3. Results and discussion

3.1. Characterization of CNC reinforced keratin bioadsorbent

By using CNC as reinforcing building blocks, 3D porous spongy keratin bioadsorbent with enhanced mechanical property, high porosity and large specific surface area was fabricated. The preparation process is presented in Fig. 1. A certain amount of CNC suspension and crosslinking agent (glutaraldehyde) was added into keratin solution. After 15 min of exposure to ultrasonic,

the mixed solution was freeze-dried and crosslinked at 70 ℃to obtain CNC reinforced keratin bioadsorbent. Morphology of the CNC was characterized by FESEM and TEM as shown in Fig. S1 (A, B). It can be observed that the obtained CNC exhibited rod-like morphology with 10 nm in width and 190 nm in length. The size distribution of CNC was shown in Fig. S1 (C). The CNC possessed a narrow size distribution with a mean diameter of 187 nm, which is favorable for its homogenous distribution within polymer matrix. There are two major effect by incorporating CNC nanoparticle: (1) improve porosity and specific surface area of keratin adsorbent by suppressing its structural shrinkage; (2) improve mechanical strength of the adsorbent which is a crucial parameter for its recyclability.

The pure keratin adsorbent obtained by freeze-drying showed poor water stability which hindered its further application. Thus, in this research glutaraldehyde was used as crosslinker to react with keratin and obtain water stable keratin adsorbent. However, the freeze-dried keratin sponge showed serious structural shrinkage which was common for porous protein materials such as sponge or scaffold after chemical crosslinking (Guo et al., 2015; Park et al., 2015). The shape shrinkage would result in the collapse of the well-formed interconnected pore network which further decrease the specific surface area and porosity of the adsorbent, resulting in the dramatic decrease of the adsorption performance as shown in Fig. S2. CNC was introduced as nano-filler to improve the dimensional stability of the adsorbent. From Fig. S2 (i-l), it is clearly observed that the dimensional stability of keratin adsorbent was highly improved after incorporation of CNC. The improvement in structural integrity and 3D dimension stability is mainly contributed to the reinforcing effect of CNC dispersed within the skeleton of keratin sponge. Morphology of the adsorbent was also investigated by SEM as shown in Fig. S3. Pore structure of the CNC reinforced keratin adsorbent after crosslinking was almost the same as that

of before crosslinking as the result of improved dimensional stability. This is also beneficial and crucial for the improvement of the adsorption performance of keratin adsorbent since the porosity and specific surface area of the CNC reinforced adsorbent is much higher than that of non-reinforced one as listed in Table S2.

Mechanical properties of the adsorbent are crucial for its regeneration and recycling. To highlight the reinforcement effects of CNC nanofiller in keratin adsorbent, the mechanical property of CNC reinforced and non-reinforced adsorbent was measured. Pure keratin adsorbent (without CNC and chemical crosslinking) were too weak for mechanical property measurement. The compression test depicted the remarkable reinforcing effect of CNC nanofiller as displayed in Fig. 2A. The compression stress of the CNC reinforced adsorbent was 1.26 times higher than that of non-reinforced one, suggesting that the incorporation of CNC as reinforcing building blocks could provide better mechanical integrity of keratin adsorbent. The reinforcing mechanism is mainly due to the formation of percolation network within keratin skeleton resulted from the homogeneous dispersion of CNC nano-particles with many point-to-point connections. The well-structured percolation network of CNC lead to a more intense energy dissipative processes resulted from the rearrangement of CNC-keratin interfacial hydrogen bonds upon deformation, thus resulting in the decreased of stress concentration and increasing resistance against crack propagation. Obviously, the CNC reinforced adsorbent possesses good structure integrity tenacity and mechanical strength as shown in the inset, which is strongly desirable for a reusable adsorbent. Fig. 2B showed the water uptake property of adsorbents in water at different contact time. It can be easily found that the equilibrium water uptake of the CNC reinforced adsorbent shown a significant increase comparing to that of without CNC incorporation, which was mainly attributed to (1) high porosity of CNC reinforced adsorbent; (2)

more functional group of -OH on CNC reinforced adsorbent; The equilibrium water uptake of the CNC reinforced adsorbent was found to be in the range of 514.6−520.4 g g^{-1}, which makes the adsorbent with excellent swelling behavior. The carboxylic and amine group contents on the CNC reinforced keratin adsorbent were 26 mmol g^{-1} and 17 mmol g^{-1} determined by conductivity titration, respectively.

3.2. Adsorption properties of CNC reinforced keratin adsorbent

Generally speaking, the physical properties and constituents of an adsorbent show a significant influence on its adsorption performance. The adsorption capacities (q_e) of keratin adsorbent with and without CNC reinforcement toward RB5 and DR80 are shown in Fig. S4. Obviously, the adsorption capacity of CNC reinforced keratin adsorbent is much higher than that of keratin adsorbent. The pH of dye solution is a dominant parameter that control the whole adsorption process as it can affect the surface property of the adsorbent as well as the ionization degree of dye molecules. The adsorption results of RB5 and DR80 by CNC reinforced keratin adsorbent as a function of pH are shown in Fig. 3. The removal efficiency (R%) and adsorption capacity (q_e) of the adsorbent decreased slowly with the increase of pH from 2 to 11. The maximum removal efficiency of the adsorbent for RB5 and DR80 was 96% and 98% at pH 2, respectively. The pH value at zero potential point (pH_{PZC}) of the adsorbent is around 5.6 (Fig. 3C). In acidic solution (pH < 5.6), the adsorbent was protonated, thus shows affinity toward dyes through electrostatic interaction. With increased pH, the adsorbent was deprotonated gradually and the adsorbent surface became more negative charged thus weakening the electrostatic attraction between the adsorbent and dye molecules. Under this circumstance, the electrostatic repulsion between dye molecules and the adsorbent would govern the adsorption process. Consequently, the adsorbent showed little affinity towards dye molecules and result in a relatively low removal efficiency for

RB5 and DR80. We can conclude that the electrostatic interaction between the adsorbent and dye molecules play a key factor in governing the adsorption process but not the only driving force for dye adsorption.

Effect of adsorbent dosage and ionic strength on the removal efficiency and adsorption capacity of dye by CNC reinforced keratin adsorbent was given in Fig. S5. The removal efficiency increased dramatically with increasing of adsorbent dosage, which was attributed to the fact that more adsorption sites were available on keratin adsorbent. The decrease of % adsorption by increasing adsorbent dosage could be explained by the fact that the amount of dye adsorbed onto unit weight of adsorbent reduced. As shown in Fig. S5C, the removal efficiency for RB5 and DR80 decreased slowly with the increase of NaCl concentration from 0 to 70 g L^{-1}. This phenomenon was mainly attributed to the competitive effect between Cl^- and the dye molecules to the adsorption sites on keratin adsorbent.

3.3. Adsorption isotherms and kinetics

Adsorption isotherm is a useful tool for evaluation of the adsorption capacity of an adsorbent as well as provide fundamental information about the adsorption behavior and the nature of the adsorbent-adsorbate interaction. Therefore, Langmuir and Freundlich isotherm models are applied to investigate the adsorption behavior. The results are shown in Fig. 4 (C) and (D) and their corresponding parameters are in Table 1. Compared with Freundlich isotherm model, the Langmuir isotherm is considered more favorable to describe the adsorption behavior for both RB5 and DR80, owing to the high correlation coefficient as shown in Table 1 ($R^2 > 0.99$), revealing that the adsorption of RB5 and DR80 on the keratin-based bioadsorbents was a homogeneous surface with monolayer sorption. The calculated q_{max} from Langmuir isotherm model was 1250 mg g^{-1} for RB5 and 1111 mg g^{-1} for DR80, respectively, suggesting that the

adsorbent demonstrates high adsorption capacity for both dyes. Also the calculated q_{max} from Langmuir model is highly close to the experimental equilibrium adsorption capacity, which further confirmed that Langmuir adsorption isotherm is favorable. The R_L was found to be in the range of 0.026-0.263 for RB5 and 0.017-0.188 for DR80 at an initial concentration from 100-1300 mg L^{-1}, which indicates that the Langmuir isotherm type is favorable ($0 < R_L < 1$).

The adsorption kinetics, which can show the evolution process of an adsorbate migrated from solution onto the adsorbent, could provide fundamental information to understand the types of adsorption process as well as explore the rate limiting step involved (Crini, 2003; Lu and Gibb, 2008). Herein, the pseudo-first-order and pseudo-second-order models were employed to investigate the adsorption process and the results are shown in Fig. 4 (E)(F), and their corresponding parameters are listed in Table 2. It is evident that the pseudo-second order model provide a better description of the kinetics of the adsorption owing to the high R^2 (**>** 0.99) values for both RB5 and DR80 in Table 2. Moreover, from Table 2, the calculated q_e from the pseudo-second order model matches well with the experimental q_{exp} for both dyes, which further confirms the validity of this model. This result indicated that the adsorption process is dependent on the amount of dyes adsorbed on the surface of keratin adsorbent and the amount adsorbed at equilibrium, suggesting that the adsorption of RB5 and DR80 onto the CNC reinforced keratin adsorbent might be chemisorption including valence forces through sharing or exchanging of electrons between adsorbent and adsorbate.

3.4. Recyclability and fixed column adsorption properties of the adsorbent

Generally, high desorption efficiency after adsorption and good reusability are desirable for an ideal adsorbent. The regeneration of the keratin adsorbent was performed by immersing the adsorbent into NaOH solution for 30 min with squeeze. Recyclability of the adsorbent was

shown in Fig. 5. Although adsorption performance of RB5 and DR80 decreased slightly, the removal efficiency of the adsorbent for RB5 and DR80 was still more than 80% after five cycles. This demonstrated that the keratin adsorbent had good recycling ability when removing RB5 and DR8.

The potential of the keratin-based bioadsorbents in practical application for dye removal was studied in continuous flow fixed-bed column and the results are shown in Fig. 5 (B) and (C). The shape of the breakthrough curve and breakthrough volume, as shown in Fig. 5B, are important characteristics for the process design of the column adsorption as well as evaluating the feasibility of the adsorbent. From Fig. 5B we can see that the breakthrough volume in which the C_t/C_0 of above 0.1 was 220 mL, and the accumulated volume was 900 mL when C_t/C_0 is above 0.9. This result indicated that the treatment volume of the dye aqueous solution reached nearly 250 mL and dye concentration in the effluent was below 20 mg L^{-1}, completely satisfying the discharge standard for industrial dye wastewater. As shown in Fig. 5C, the in situ desorption of dye from the fixed bed can be easily realized by the elution with 1% wt NaOH and even could obtain a concentrated dye solution. The dye concentration in the first 25 mL eluent was measured to be around 510 mg L^{-1}, and the adsorbed dye can be concentrated into a solution with nearly 3 times of that initial concentration of dye solution, suggesting that the fixed bed can be regenerated via in situ desorption and reuse again. Considering such small amount (0.35 g) of the CNC reinforced keratin adsorbent packed in the fixed-bed column, it can be predicted that the breakthrough volume would become larger with the increase in the filling amount of the adsorbent.

3.5. Adsorption mechanism of dyes by the adsorbent

In general, both physical structure and chemical composition of the adsorbent show significant influence on the adsorption performance. From the physical structure characterization, we know that the adsorbent exhibit large specific surface area and high porosity which make it possible for the adsorbent to interact with dye molecules sufficiently. Meanwhile, CNC reinforced keratin adsorbent has an interconnected pore structure, which allowing dye molecules diffusion into the inner part of the adsorbent. Furthermore, it is worth mentioning that the unique flexible pore structure of the adsorbent is crucial for the desorption process. The pores were compressed under squeeze and dye molecules that were adsorbed inside of those pores under weak attraction force could be squeezed out and desorbed into the effluent. In the meantime, dye molecules that were adsorbed onto the adsorbent could migrate into the inner pores of the adsorbent as the result of concentration differential. Consequently, dye molecules were desorbed gradually. Finally, the abundant functional groups such as hydroxyl, carboxyl and amino group on the adsorbent is another important factor that contributing to its excellent adsorption performance. From the study of pH and zeta potential effect on adsorption efficiency we could conclude that the electrostatic interaction played a major role in the adsorption of dye molecules by CNC reinforced keratin adsorbent and, as well known, the $-NH_2$, -OH groups could also facilitate dye diffusion and adsorption process via the formation of hydrogen bonds or van der Waals forces. Thus, as shown in Fig. 6, we proposed the adsorption mechanism of RB5 and DR80 by the adsorbent based on above discussions.

4. Conclusions

A novel 3D keratin bioadsorbent reinforced by CNC was successfully prepared and it exhibited excellent dye removal performance, which was mainly attributed to the high porosity (99.8%), large specific surface area (229 $m^2 g^{-1}$) and abundant of adsorption sites on the adsorbent. The

regeneration and recyclability results demonstrated that the adsorbent possessed good reusability. In addition, the fixed bed column study revealed that the adsorbent had excellent performance for dye wastewater treatment. This work could not only provide a new perspective for development of high performance adsorbent but also could explore the value added way to application of waste biomass.

Acknowledgements

This research was financially supported by USDA-National Institute of Food and Agriculture (Multi-State Project S1054 (NEB 37-037)), USDA Hatch Act, and the Agricultural Research Division at the University of Nebraska-Lincoln. Authors are grateful to China Scholarship Council for providing financial support to Kaili Song.

References

1. Achak, M., Hafidi, A., Ouazzani, N., Sayadi, S., Mandi, L., 2009. Low cost biosorbent "banana peel" for the removal of phenolic compounds from olive mill wastewater: Kinetic and equilibrium studies. J. Hazard. Mater. 166, 117–125.
2. Aluigi, A., Rombaldoni, F., Tonetti, C., Jannoke, L., 2014. Study of Methylene Blue adsorption on keratin nanofibrous membranes. J. Hazard. Mater. 268, 156–165.
3. Bilal, M., Shah, J.A., Ashfaq, T., Gardazi, S.M.H., Tahir, A.A., Pervez, A., Haroon, H., Mahmood, Q., 2013. Waste biomass adsorbents for copper removal from industrial wastewater--a review. J. Hazard. Mater. 263, 322–33.
4. Cao, J.S., Lin, J.X., Fang, F., Zhang, M.T., Hu, Z.R., 2014. A new absorbent by modifying walnut shell for the removal of anionic dye: kinetic and thermodynamic studies. Bioresour. Technol. 163, 199–205.
5. Cazetta, A.L., Pezoti, O., Bedin, K.C., Silva, T.L., Junior, Andrea Paesano Asefa, T., Almeida, V.C., 2016. Magnetic activated carbon derived from biomass waste by concurrent synthesis: efficient adsorbent for toxic dyes. ACS Sustain. Chem. Eng. 4, 1058-1068.
6. Crini, G., 2006. Non-conventional low-cost adsorbents for dye removal : A review. Bioresour. Technol. 97, 1061–1085.
7. Crini, G., 2003. Studies on adsorption of dyes on beta-cyclodextrin polymer. Bioresour. Technol. 90, 193–198.
8. González, J.A., Villanueva, M.E., Piehl, L.L., Copello, G.J., 2015. Development of a chitin/graphene oxide hybrid composite for the removal of pollutant dyes: adsorption and desorption study. Chem. Eng. J. 280, 41–48.

9. Guo, J., Pan, S., Yin, X., He, Y.F., Li, T., Wang, R.M., 2015. PH-sensitive keratin-based polymer hydrogel and its controllable drug-release behavior. J. Appl. Polym. Sci. 132, 1–8.
10. Gupta, V.K., Suhas, 2009. Application of low-cost adsorbents for dye removal - A review. J. Environ. Manage. 90, 2313–2342.
11. Huang, M., Tunnicliffe, L.B., Zhuang, J., Ren, W., Yan, H., Busfield, J.J.C., 2016. Strain-dependent dielectric behavior of carbon black reinforced natural rubber. Macromolecules 49, 2339–2347
12. Lin, L., Zhai, S.R., Xiao, Z.Y., Song, Y., An, Q. D., Song, X.W., 2013. Dye adsorption of mesoporous activated carbons produced from NaOH-pretreated rice husks. Bioresour. Technol. 136, 437–443.
13. Lin, N., Bruzzese, C., Dufresne, A., 2012. TEMPO-oxidized nanocellulose participating as crosslinking aid for alginate-based sponges. ACS Appl. Mater. Interfaces 4, 4948–4959.
14. Liu, X., Lee, D.J., 2014. Thermodynamic parameters for adsorption equilibrium of heavy metals and dyes from wastewaters. Bioresour. Technol. 160, 24–31.
15. Liu, Y., Jiang, Y., Hu, M., Li, S., Zhai, Q., 2015. Removal of triphenylmethane dyes by calcium carbonate-lentinan hierarchical mesoporous hybrid materials. Chem. Eng. J. 273, 371–380.
16. Lu, S., Gibb, S.W., 2008. Copper removal from wastewater using spent-grain as biosorbent. Bioresour. Technol. 99, 1509–1517.
17. Maneerung, T., Liew, J., Dai, Y., Kawi, S., Chong, C., Wang, C.H., 2016. Activated carbon derived from carbon residue from biomass gasification and its application for dye

adsorption: kinetics, isotherms and thermodynamic studies. Bioresour. Technol. 200, 350–359.

18. Mittal, A., Kurup, L., Mittal, J., 2007. Freundlich and Langmuir adsorption isotherms and kinetics for the removal of tartrazine from aqueous solutions using hen feathers. J. Hazard. Mater. 146, 243–248.
19. Mittal A.a Thakur, V.. M.J.. V.H., 2014. Process development for the removal of hazardous anionic azo dye congo red from wastewater by using hen feather as potential adsorbent. Desalin. Water Treat. 52, 227–237.
20. Nair, V., Vinu, R., 2016. Peroxide-assisted microwave activation of pyrolysis char for adsorption of dyes from wastewater. Bioresour. Technol. 216, 511–519.
21. Pal, S., Patra, A.S., Ghorai, S., Sarkar, A.K., Mahato, V., Sarkar, S., Singh, R.P., 2015. Efficient and rapid adsorption characteristics of templating modified guar gum and silica nanocomposite toward removal of toxic reactive blue and congo red dyes. Bioresour. Technol. 191, 291–299.
22. Papić, S., Koprivanac, N., Lončarić Božić, A., Meteš, A., 2004. Removal of some reactive dyes from synthetic wastewater by combined Al(III) coagulation/carbon adsorption process. Dye. Pigment. 62, 291–298.
23. Park, M., Shin, H.K., Kim, B.S., Kim, M.J., Kim, I.S., Park, B.Y., Kim, H.Y., 2015. Effect of discarded keratin-based biocomposite hydrogels on the wound healing process in vivo. Mater. Sci. Eng. C 55, 88–94.
24. Pei, A., Butchosa, N., Berglund, L. a., Zhou, Q., 2013. Surface quaternized cellulose nanofibrils with high water absorbency and adsorption capacity for anionic dyes. Soft Matter 9, 2047.

25. Qin, Y., Wang, L., Zhao, C., Chen, D., Ma, Y., Yang, W., 2016. Ammonium-functionalized hollow Polymer particles as a pH-responsive adsorbent for selective removal of acid dye. ACS Appl. Mater. Interfaces 8, 16690–16698.
26. Renault, F., Morin-Crini, N., Gimbert, F., Badot, P.M., Crini, G., 2008. Cationized starch-based material as a new ion-exchanger adsorbent for the removal of C.I. Acid Blue 25 from aqueous solutions. Bioresour. Technol. 99, 7573–7586.
27. Sewu, D.D., Boakye, P., Woo, S.H., 2016. Highly efficient adsorption of cationic dye by biochar produced with korean cabbage waste. Bioresour. Technol. 224, 206–213.
28. Song, K., Gao, A., Cheng, X., Xie, K., 2015. Preparation of the superhydrophobic nano-hybrid membrane containing carbon nanotube based on chitosan and its antibacterial activity. Carbohydr. Polym. 130, 381–387.
29. Song, K., Xu, H., Xie, K., Yang, Y., 2016. Effects of chemical structures of polycarboxylic acids on molecular and performance manipulation of hair keratin. RSC Adv. 6, 58594–58603.
30. Song, W., Gao, B., Xu, X., Xing, L., Han, S., Duan, P., Song, W., Jia, R., 2015. Adsorption-desorption behavior of magnetic amine/Fe_3O_4 functionalized biopolymer resin towards anionic dyes from wastewater. Bioresour. Technol. 210, 123–130.
31. Tao, J., Xiong, J., Jiao, C., Zhang, D., Lin, H., Chen, Y., 2016. Hybrid mesoporous silica based on hyperbranch-substrate nanonetwork as highly efficient adsorbent for water treatment. ACS Sustain. Chem. Eng. 4, 60–68.
32. Wang, H., Wang, C., Tao, S., Qiu, J., Yu, Y., Gu, M., 2016. Biomimetic Preparation of hybrid porous adsorbents for efficiently purifying complex wastewater. ACS Sustain. Chem. Eng. 4, 992-998.

33. Xu, H., Cai, S., Xu, L., Yang, Y., 2014. Water-stable three-dimensional ultrafine fibrous scaffolds from keratin for cartilage tissue engineering. Langmuir 30, 8461-8470.

34. Xu, H., Yang, Y., 2014. Controlled de-cross-linking and disentanglement of feather keratin for fiber preparation via a novel process. ACS Sustain. Chem. Eng. 2, 1404–1410.

35. Xu, H., Zhang, Y., Jiang, Q., Reddy, N., Yang, Y., 2013. Biodegradable hollow zein nanoparticles for removal of reactive dyes from wastewater. J. Environ. Manage. 125, 33-40.

36. Yang, L., Phua, S.L., Teo, J.K.H., Toh, C.L., Lau, S.K., Ma, J., Lu, X., 2011. A biomimetic approach to enhancing interfacial interactions: Polydopamine-coated clay as reinforcement for epoxy resin. ACS Appl. Mater. Interfaces 3, 3026–3032.

37. Yao, T., Guo, S., Zeng, C., Wang, C., Zhang, L., 2015. Investigation on efficient adsorption of cationic dyes on porous magnetic polyacrylamide microspheres. J. Hazard. Mater. 292, 90–97.

38. Zhang, S., Gao, H., Li, J., Huang, Y., Alsaedi, A., Hayat, T., Xu, X., Wang, X., 2017. Rice husks as a sustainable silica source for hierarchical flower-like metal silicate architectures assembled into ultrathin nanosheets for adsorption and catalysis. J. Hazard. Mater. 321, 92–102.

39. Zhang, W., Li, H., Kan, X., Dong, L., Yan, H., Jiang, Z., Yang, H., Li, A., Cheng, R., 2012. Adsorption of anionic dyes from aqueous solutions using chemically modified straw. Bioresour. Technol. 117, 40–47.

40. Zhao, F., Repo, E., Yin, D., Meng, Y., Jafari, S., Sillanpää, M., 2015. EDTA-Cross-Linked β-cyclodextrin: an environmentally friendly bifunctional adsorbent for simultaneous adsorption of metals and cationic dyes. Environ. Sci. Technol. 49, 10570–

10580.

41. Zou, Y., Huda, S., Yang, Y., 2010. Lightweight composites from long wheat straw and polypropylene web. Bioresour. Technol. 101, 2026–2033.

Figure captions

Fig. 1. Schematic illustration of the preparation of CNC reinforced keratin bioadsorbent.

Fig. 2. Mechanical strength (A) and water uptake property (B) of the prepared CNC reinforced keratin bioadsorbent and bioadsorbent without CNC.

Fig. 3. Effect of pH on Removal efficiency and Adsorption capacity of (A) RB5 and (B) DR80 by CNC reinforced keratin adsorbent (initial dye concentration: 200 mg L^{-1}, 200 mL dye solution, 0.1g adsorbent); (C) Zeta potential of CNC reinforced keratin adsorbent at different pH values.

Fig. 4. Effect of initial dye concentration (C_0) on removal efficiency and adsorption capacity of (A) RB5 and (B) DR80 (dye solution pH=2, 200mL dye solution, 0.1g adsorbent); Adsorption isotherm of (C) RB5 and (D) DR80 at room temperatures; Adsorption kinetics of (E) RB5, (F) DR80 by the adsorbent.

Fig. 5. (A) Recycle study of the adsorbent in removal of dyes (dye solution pH=2, 200mL dye solution with 200 mg L^{-1} dye concentration, 0.1g adsorbent); Breakthrough curve of the adsorbent in removal of RB5 (B) and the dynamic desorption performance (C) of the adsorbed bed.

Fig. 6. Schematic adsorption mechanism of dye molecules by CNC reinforced keratin adsorbent.

Table 1

Isothermic Parameters for the Adsorption of RB5 and DR80 by CNC reinforced keratin adsorbent.

	Langmuir isotherm			Freundlich isotherm		
	b (L mg^{-1})	q_{max} (mg g^{-1})	R^2	K_f (L mg^{-1})	n	R^2
RB5	0.028	1250	0.9925	156.78	3.03	0.9759
DR80	0.043	1111	0.9946	186.84	3.56	0.9436

Table 2

Kinetic Parameters of Pseudo-First-Order and Pseudo-Second-Order models for the Adsorption of RB5 and DR80 by keratin adsorbent.

		Pseudo-First-Order			Pseudo-Second-Order		
	q_{exp}(mg g^{-1})	k_1 (min^{-1})	q_e (mg g^{-1})	R^2	k_2 (g $mg^{-1}min^{-1}$)	q_e (mg g^{-1})	R^2
RB5	475	0.0173	727	0.9609	$2.16*10^{-5}$	588	0.9924
DR80	485	0.0138	521	0.98	$3.05*10^{-5}$	555	0.9948

Table 3

Comparison of adsorption capacity of textile dyes by some keratin-based adsorbents and other adsorbents.

Adsorbent	Dye	q_e (mg g^{-1})	Recycle	Reference
Hen feather	Congo red	172	Not done	(Mittal A.a Thakur, 2014)
Hen feather	Tartrazine	80	Not done	(Mittal et al., 2007)
Keratin nano-membrane	Methylene blue	170	Not done	(Aluigi et al., 2014)
Modified straw	Methyl orange	300	Not done	(Zhang et al., 2012)
	Acid green	950		
Quaternized nano-cellulose	Acid green 25	683	Not done	(Pei et al., 2013)
	Congo red	664		
Modified walnut shell	Reactive brilliant red	568	198mg g^{-1} at the 5th recycle	(Cao et al., 2014)
Wood chip biochar	Congo red	110	Not done	(Sewu et al., 2016)
Korean cabbage biochar		95.81		
Rice Straw biochar		190.8		
Activated carbon		449.1		
Activated carbon	Rhodamine B	189.8	Not done	(Maneerung et al., 2016)
Keratin adsorbent	Reactive black 5	1250	1000 mg g^{-1} at the 5th recycle	This study
	Direct red 80	1111	890 mg g^{-1} at the 5th recycle	

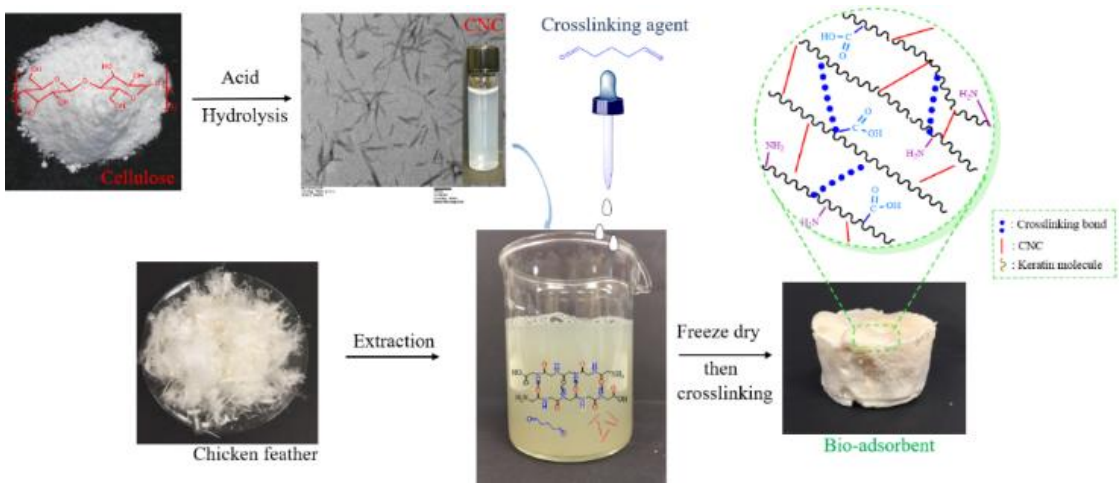

Fig. 1. Schematic illustration of the preparation of CNC reinforced keratin bioadsorbent.

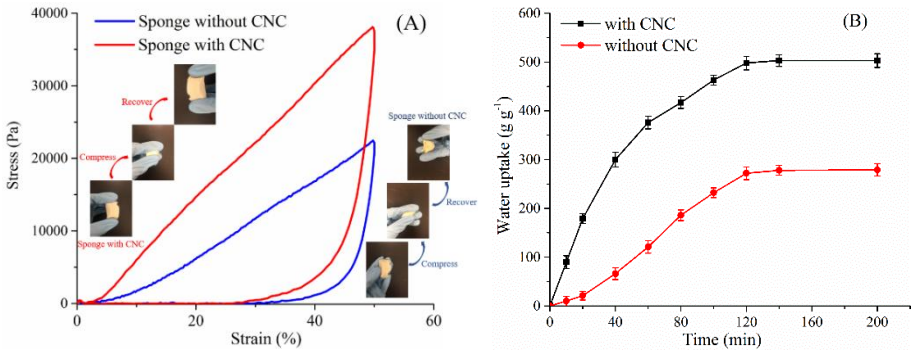

Fig. 2. Mechanical strength (A) and water uptake property (B) of the prepared CNC reinforced keratin bioadsorbent and bioadsorbent without CNC.

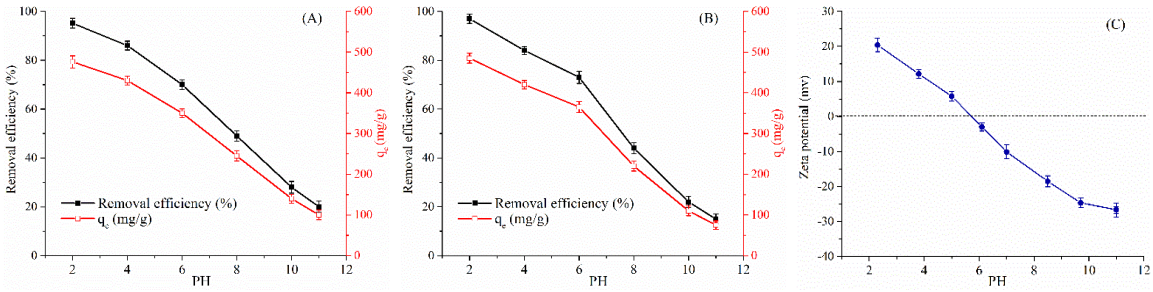

Fig. 3. Effect of pH on Removal efficiency and Adsorption capacity of (A) RB5 and (B) DR80 by CNC reinforced keratin adsorbent (initial dye concentration: 200 mg L^{-1}, 200 mL dye solution, 0.1g adsorbent); (C) Zeta potential of CNC reinforced keratin adsorbent at different pH values.

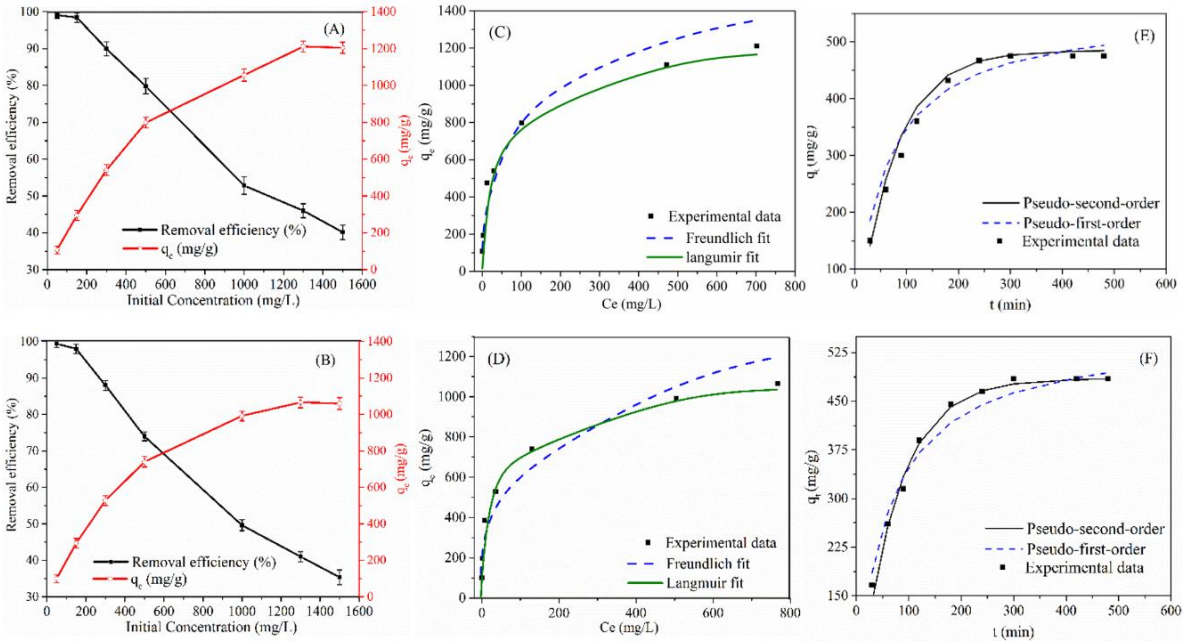

Fig. 4. Effect of initial dye concentration (C_0) on removal efficiency and adsorption capacity of (A) RB5 and (B) DR80 (dye solution pH=2, 200mL dye solution, 0.1g adsorbent); Adsorption isotherm of (C) RB5 and (D) DR80 at room temperatures; Adsorption kinetics of (E) RB5, (F) DR80 by the adsorbent.

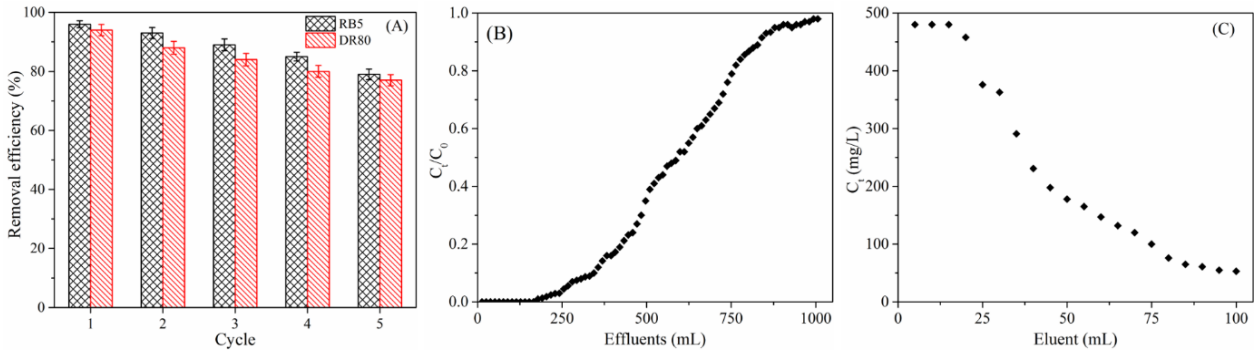

Fig. 5. (A) Recycle study of the adsorbent in removal of dyes (dye solution pH=2, 200mL dye solution with 200 mg L^{-1} dye concentration, 0.1g adsorbent); Breakthrough curve of the adsorbent in removal of RB5 (B) and the dynamic desorption performance (C) of the adsorbed bed.

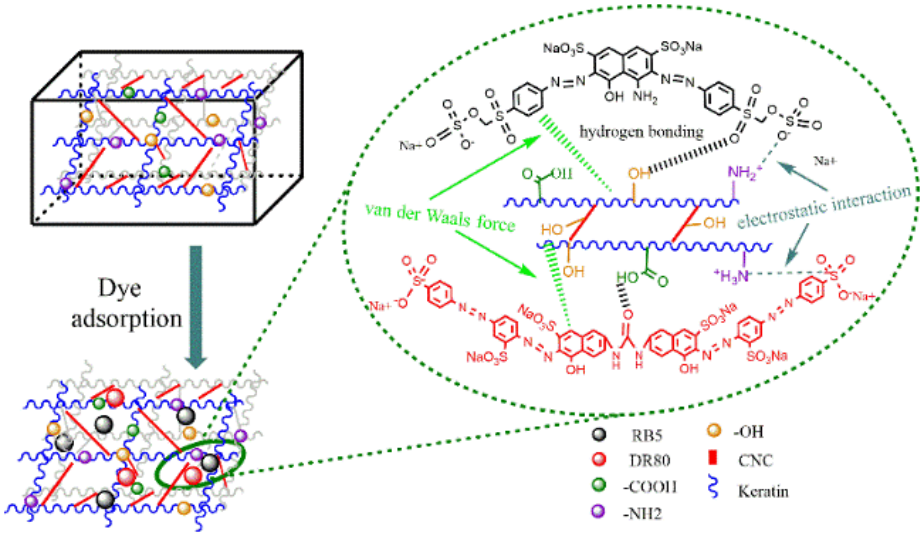

Fig. 6. Schematic adsorption mechanism of dye molecules by CNC reinforced keratin adsorbent.

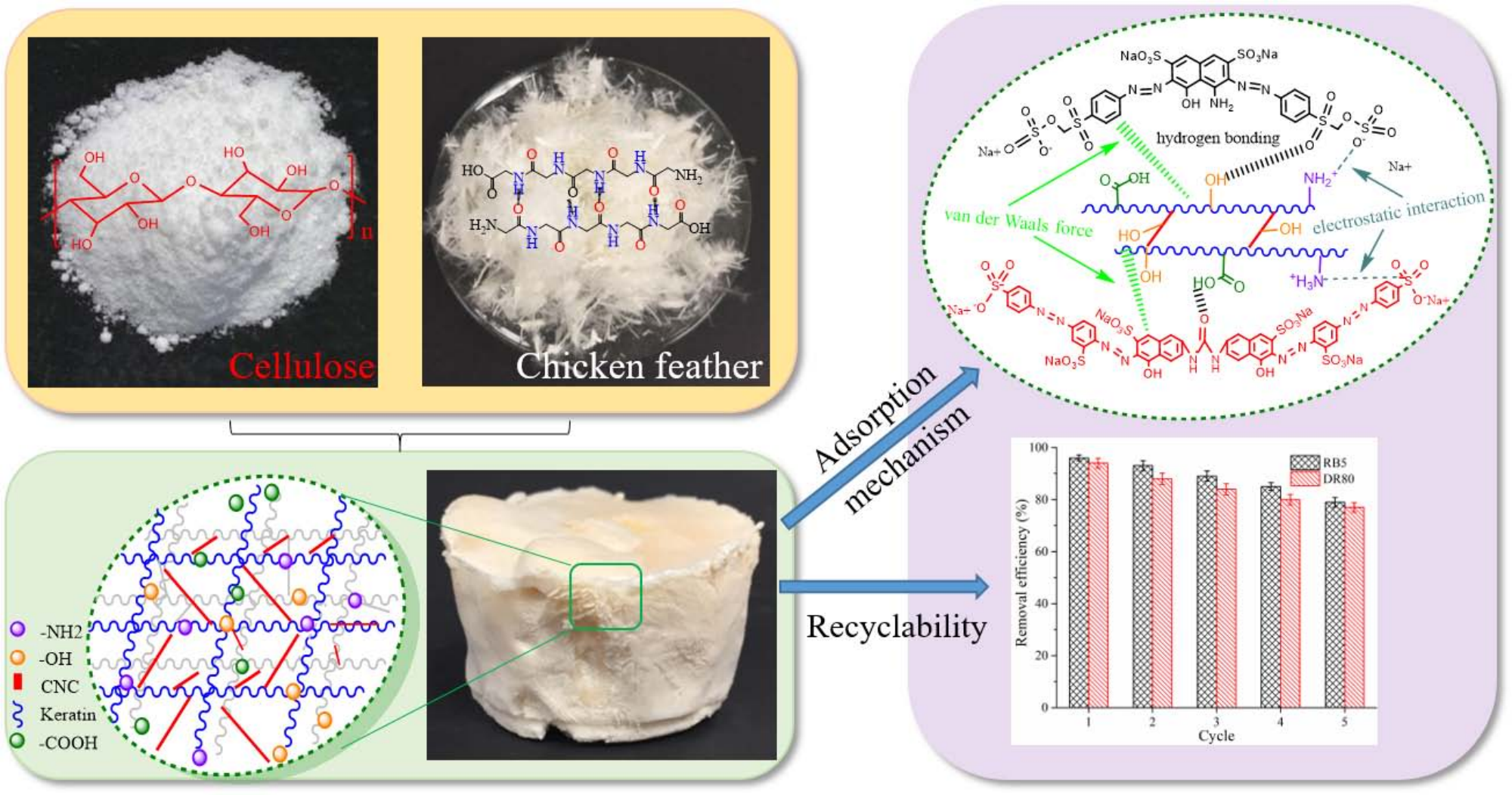
Cellulose
Chicken feather
-NH2
-OH
CNC
Keratin
-COOH
Adsorption mechanism
Recyclability
hydrogen bonding
van der Waals force
electrostatic interaction
RB5
DR80
Removal efficiency (%)
Cycle